

Voltage-biased I-V characteristics in the multi-Josephson junction model of high T_c superconductors

Shoichi SAKAMOTO and Hideki MATSUMOTO

Department of Applied Physics, Seikei University

Kichijoji Kitamachi 3-3-1

Musashino-shi, 180-8633 JAPAN

and

Tomio KOYAMA

Institute for Materials Research, Tohoku University

Katahira 2-1-1, Sendai, 980 JAPAN

and

Masahiko MACHIDA

Center for Promotion of Computational Science and Engineering

Japan Atomic Research Institute

2-2-54 Nakameguro, Meguro-ku, Tokyo, 153 JAPAN

September 20, 2018

Abstract

By use of the multi-Josephson junction model, we investigate voltage-biased I-V characteristics. Differently from the case of the single junction, I-V characteristics show a complicated behavior due to inter-layer couplings among superconducting phase differences mediated by the charging effect. We show that there exist three characteristic regions, which are identified by jumps and cusps in the I-V curve. In the low voltage region, the total current is periodic with trigonometric functional increases and rapid drops. Then a kind of chaotic region is followed. Above certain voltage, the total current behaves with a simple harmonic oscillation and the I-V characteristics form a multi-branch structure as in the current-biased case. The above behavior is the result of the inter-layer coupling, and may be used to confirm the inter-layer coupling mechanism of the formation of hysteresis branches.

1 Introduction

I-V characteristics of the high T_c superconductor $\text{Bi}_2\text{Sr}_2\text{Ca}_1\text{C}_2\text{O}_8$ (BSCCO) shows a strong hysteresis, producing multi-branches [1, 2, 3]. Many experiments have been reported to

investigate properties of hysteresis branches [4, 5, 6, 7, 8, 9, 10], and it has turned out that there is rich physics in properties of I-V characteristics. Substructures are found in hysteresis branches, and are discussed in relation with phonon effects [8]. The d-wave effect is also discussed in the higher voltage region, where the tunneling current becomes important [6, 10].

It is well known in a single Josephson junction that the application of a constant voltage-bias leads a rather simple phenomenon of the harmonic current-oscillation with the frequency proportional to the applied voltage [11]. This is due to the fact that the time-derivative of the phase difference is directly connected with the voltage, and that there is no room for the phase to move freely. Therefore, the most of the above mentioned experiments were performed with the current biased arrangement, aiming to investigate properties of I-V hysteresis branches, and, as long as we know, no systematic experiment with the voltage bias has been reported. We will point out in this paper that anomalous behaviors are expected, theoretically, in the low voltage-biased region in the case of the multi-layered intrinsic Josephson junctions of high T_c superconductors, and that the voltage-biased experiment gives additional information on behaviors of I-V characteristics.

In the multi-layered intrinsic Josephson junctions of high T_c superconductors, inter-layer couplings among superconducting phase differences become important due to the atomic scale of the thickness of the superconducting layer. In the ref. [12] the mechanism of the inter-layer coupling is proposed as the charging effect of superconducting layers; the charging effect induces the variation of electric field and mediates the inter-layer coupling among superconducting phase differences. It has been shown that, by this mechanism, a branch structure in the I-V characteristics is obtained as the intrinsic nature of the strong anisotropy of high T_c superconductors [13]. In the previous paper [14], we have investigated the origin of hysteresis branches, and have shown that hysteresis jumps are induced when solutions change in nonlinear-coupled equations of phase-differences. Namely, the number of rotating phases and its patterns classifies solutions. At a point of a hysteresis jump, its number or distribution pattern is changed.

The main difference between the cases of the single junction and the multi-junction lies in the fact that the applied voltage gives restriction only on the total voltage. Therefore, each junction may behave in a self-adjusted way, if an interaction effect allows it. In a simple array of N single junctions, each junction feels only the N -th of the applied voltage, and one cannot expect much difference from the case of the single junction. However, in the intrinsic Josephson array of the high T_c superconductors, the existence of an inter-layer coupling affects the collective motion of phase differences. Furthermore, the voltage control and current control lead different situations. Specially, in the voltage control case, one can reach transient unstable states of the current biased case, since the applied voltage still enforces the total behavior of phase differences. In this paper, we investigate I-V characteristics in voltage-biased cases of high T_c superconductors. Since there is no experiment available to refer at present, several cases with possible surface conditions will be presented.

In the next section, we summarize the formula for the voltage-biased case in the multi-Josephson junction model. In Sect. 3, we present numerically simulated results, and present I-V characteristics of the voltage-biased case. It will be shown that certain anomalous behavior of I-V characteristics appears in the applied low voltage region. We show that the voltage region is divided roughly into three regions, an anomalous periodic region, a chaotic region and a region of hysteresis branches. In an anomalous periodic region, the current shows a trigonometric functional increase and rapid drop. In a chaotic region, the total current behaves chaotically. In the last region, the behavior of the current is quasi-harmonic. Physical origin of these regions will be discussed. Sect. 4 is devoted to concluding remarks.

2 Formula for the voltage biased multi-Josephson junction

In this section, we rewrite the formula for the multi-Josephson junction of ref. [14] suitable to the voltage-biased analysis. The notations used here are same as those in ref. [14]. Namely, we consider the $N + 1$ superconducting layers, numbered from 0 to N . We denote the gauge invariant phase difference of the $(l - 1)$ -th and l -th superconducting layer by $\varphi(l)$, and voltage by $V(l)$. The widths of the insulating and superconducting layers are denoted by D and s , respectively. At the edges, the effective width of the superconducting layer may be extended due to the proximity effect into attached lead metals. The widths of the 0-th and N -th superconducting layers are denoted by s_0 and s_N , respectively.

In the voltage-biased case, the total voltage is equal to the applied external voltage V_{ext} ,

$$V_{ext} = \sum_{l=1}^N V_l . \quad (1)$$

In order to perform a numerical simulation under the condition (1), we rewrite the equation for the total current J (Eq. (1) in ref. [14]) and the equation relating the time-derivative of phase-difference and voltage (Eq. (3) in ref. [14]) in the following way. First, we note that the total current J is expressed by the external voltage V_{ext} as

$$\frac{J}{J_c} = \frac{1}{N} \left(\sum_{l=1}^N j_c(l) \sin(\varphi(l)) + \beta \frac{V_{ext}}{V_p} + \frac{1}{\omega_p} \frac{\partial V_{ext}}{\partial t} \frac{1}{V_p} \right) . \quad (2)$$

The current J is normalized by the critical current J_c , $j_c(l) = J_c(l)/J_c$ with $J_c(l)$ being the critical current for the l -th junction. The time t is normalized by the inverse of the plasma frequency, $\omega_p = \sqrt{\frac{2e}{\hbar} \frac{4\pi D J_c}{\epsilon}}$, with ϵ being dielectric constant of the insulating layer. The voltage $V(l)$ is normalized by $V_p = \frac{\hbar \omega_p}{2e}$. The parameter β is given by $\beta = \frac{\sigma V_p}{J_c D}$. We define the voltage difference $v(l)$ as

$$V(l) = \frac{1}{N} V_{ext} + v(l) . \quad (3)$$

Then we have the following coupled differential equations,

$$\frac{1}{\omega_p} \frac{\partial v(l)}{\partial t} \frac{1}{V_p} = -\beta \frac{v(l)}{V_p} - j_c(l) \sin(\varphi(l)) + \frac{1}{N} \sum_{l'=1}^N j_c(l') \sin(\varphi(l')) \quad (4)$$

and

$$\frac{1}{\omega_p} \frac{\partial \varphi(l)}{\partial t} = \sum_{l'=1}^N A_{ll'} \left(\frac{1}{N} \frac{V_{ext}}{V_p} + \frac{v(l')}{V_p} \right). \quad (5)$$

A dissipation effect[14, 15, 16]in superconducting layers will be neglected in this paper, and the matrix A is given in Eq. (4) in ref. [14]. It should be noted that Eq. (4) gives

$$\frac{1}{\omega_p} \frac{\partial}{\partial t} \sum_{l=1}^N v(l) = -\beta \sum_{l=1}^N v(l). \quad (6)$$

Therefore if

$$\sum_{l=1}^N v(l) = 0 \quad (7)$$

is satisfied at the initial time, it is satisfied in all time. In the next section, we present results of solving Eqs. (4) and (5) by numerical simulation. The restriction from the total voltage is achieved by putting the initial condition Eq. (7). The equation for $\varphi(l)$, Eq. (5), indicates that the phase differences move according to $\frac{1}{N} V_{ext}$ as average. However, due to the mutual interaction, each $\varphi(l)$ shows a complicated behavior which affects the I-V characteristics and the behavior of the total current.

3 Results of numerical simulation

We have solved the coupled differential equations (4) and (5) by use of the fourth order Runge-Kutta method. The average current J is obtained by

$$J = \frac{1}{T_{max} - T_{min}} \int_{T_{min}}^{T_{max}} dt J(t). \quad (8)$$

We choose the parameters as $N = 10$, $\alpha = 1.0$ and $\beta = 0.2$, which has been used in ref. [14]. In the simulation we have chosen the time step $\omega_p dt = 1.0 \times 10^{-3}$, $\beta \omega_p T_{min} = 10.0$, $\beta \omega_p T_{max} = 310.0$ and the voltage step $dV_{ext} = 0.01$.

As Eq. (5) shows, the phase $\varphi(l)$ increases according to $\int dt \frac{1}{N} V_{ext}$ when V_{ext} is small. When $\varphi(l)$ reaches the value $\frac{\pi}{2}$, the phase goes into a rotating mode as can be seen from the analogy of the motion of a pendulum with a $\sin(\varphi(l))$ -nonlinear term. This indicates that the whole motions of phases $\varphi(l)$ are much affected by the phase with the lowest j_c .

It may be difficult to arrange two electrode at edges exactly in the same condition. However, in order to show how surface conditions affect the behavior of I-V characteristics, we present the following three cases; 1) $J_c(l)$ are symmetric but widths of surface are asymmetric, 2) both $J_c(l)$ and widths of surface symmetric, and 3) $J_c(l)$ asymmetric and

widths of surface symmetric. The case with $J_c(l)$ asymmetric and widths of surface asymmetric shows similar behaviors as the case 3). It should be noted that, even if the asymmetry between s_0 and s_N is introduced, the observed critical current is J_c in the current-biased case.

We first assume that all $j_c(l)$ are equal,

$$j_c(l) = 1.0 . \quad (9)$$

and choose, for example, an asymmetric boundary condition $s_0/s = 1.0$ and $s_N/s = 2.0$. In the present analysis, it is enough to have slight difference between s_0 and s_N , the difference of proximity effect.

In Fig. 1(a), we show the overall behavior of I-V characteristics obtained from the adiabatic increase and decrease of the applied voltage (circle points) and those obtained from abrupt application of the voltage (\times points). We can see that the I-V characteristics show many hysteresis jumps, forming a branch structure. In the abrupt application of voltage, the data points in the low voltage region are scattered, although they lie on some linear I-V branches. Each I-V branch is classified by a number and pattern of rotating phases. When the voltage is large enough, all junctions have the rotating phase and the single I-V characteristic is obtained. In Fig. 1(a), we notice that there exists the region where the adiabatic and abrupt applications of voltage give the same results, in the low voltage region before the branch structure starts. In Fig. 1(b), we expand the low voltage region. We can identify the obvious branches labeled as I₁, I₂, II, III₁ and III₂. The crosses (\times) are for the abrupt voltage application. The lines I and II are same for three cases of the adiabatic increase, decrease and abrupt application of the voltage. The branches III₁ and III₂ are linear. The calculation shows that the I-V relations for III₁ and III₂ are same as those obtained from the hysteresis branches in the I-V characteristics of the current-biased case. On the line III₁, the phase $\varphi(1)$ is rotating and on the line III₂ the phases $\varphi(1)$ and $\varphi(N)$ are rotating. Other phases $\varphi(l)$ are oscillating. The cross points are grouped as one rotating-phase and two-rotating phase. The scattered points are identified by the distribution of the rotating-phases among N junctions.

In Fig. 2, we show the I-V characteristics, when we choose a symmetric boundary condition $s_0/s = 1.0$ and $s_N/s = 1.0$. The branch II in Fig.1 is separated into II₁ and II₂. The branch III₂ is linear and is exactly same line as III₂ in Fig. 1. Although the branch II₂ is linear as average and lies on the same line as III₁, the calculated points are largely scattered, indicating a certain kind of instability. In order to obtain Fig. 2, we have to ensure the symmetry,

$$\varphi(l) = \varphi(N + 1 - l) , \quad V(l) = V(N + 1 - l) , \quad (10)$$

in each time step by taking the average of $\varphi(l)$ and $\varphi(N + 1 - l)$, for example. Otherwise, a very small round error rapidly develops in the region II, and we obtained the similar result of Fig. 1(b), although we start with the symmetric boundary condition.

In order to see what kinds of solutions are realized in the regions I and II, we plot, in Fig. 3, the time-dependence of the phase $\varphi(l)$ and the current J for the case of Fig. 2. Fig.

3(a),(b) are for the branches I_1 , and Fig. 3(c),(d) are for II_1 . Fig. 3(b) shows periodic current behaviors, while Fig. 3(d) shows chaotic current behaviors. The results show the following. All $\varphi(l)$ increase slowly in the same way according to the applied voltage. When $\varphi(1)$ and $\varphi(N)$ at the edges reach the value $\frac{\pi}{2}$, they increase rapidly in the phase-rotating mode. Other $\varphi(l)$'s swing back. The phases $\varphi(1)$ and $\varphi(N)$ damp their motion by the effect of resistance β , and move slowly again in the same way as other phases. As the result, the current behaves periodically with trigonometric functional increase and rapid drop. The regions I_1 and I_2 are different in the values of phase rotation, 2π and 4π , before damping. In Fig. 3(c), not only the phases at the edges but also other phases $\varphi(l)$ go into the rotating mode. Since oscillation and rotation of phases are interface in a complicated way, the chaotic current behavior is produced. The regions II_1 and II_2 are different in the values of phase rotation, 2π and 4π , at the edges.

The above results lead us the following understanding of solutions of the multi-Josephson junction in the voltage-biased case. The applied voltage V_{ext} forces the phase-differences $\varphi(l)$ of junctions to rotate. When some $\varphi(l)$ reaches $\frac{\pi}{2}$, it goes into the natural rotating mode with other phases swinging back. How much it rotates depends on its speed and resistance, forming new non-ohmic branches. When the rotation and oscillation of phase differences start to interact, solutions go into a chaotic region. When the voltage becomes large enough for certain phase difference to keep rotating, the I-V characteristics become ohmic and form multi-branches.

From the above understanding, we can immediately see that the I-V characteristics may change when there exists a certain junction with weaker j_c . Most likely, the surface layers may be damaged in the preparation process of electrodes. In fact in the previous analysis [14], we have to choose reduced J_c values at the edges in order to fit the data. It was also reported that for thin film mesa structures the preparation process for the upper electrode can produce a cut of the first junctions, leading to an area about half size and thus half critical current for those junctions [17]. As an example, we choose

$$j_c(1) = 0.5, \quad j_c(l) = 1.0 \quad (l \neq 1). \quad (11)$$

The result is presented in Fig. 4. The chaotic region II is missing. In the inset Fig. 4(b), we show the enlarged figure of the region I. There are some drops and quasi-periodic structure in the I-V characteristics. Each part has a different value of $\varphi(l)$ -phase rotation, $2\pi n$. We note that, in ref. [18], the appearance of certain periodicity in I-V characteristics has been reported, though it is for the sample of submicron junctions with no branch structures. It is a future problem to see if there is some relation with the present analysis.

We also point out that, in the analysis of Fig. 1, the regions I-II are obtained also when the external voltage is applied abruptly. Adiabatic and abrupt voltage application differ in the initial total energy. Therefore, the present result shows that the regions I-II have the single stationary state.

4 Conclusion

In this paper, we have investigated the I-V characteristics of the voltage-biased case. Differently from the case of the single junction, I-V characteristics shows the characteristic behavior originated from the mutual inter-layer coupling mediated by the charging effect. Although each junction feels as average the external voltage as $\frac{1}{N}V_{ext}$, there is a still room for each phase to move self-consistently according to the interaction. Therefore, when the voltage is low, there is a competition of the voltage forced motion and the motion induced by the interactions. Adiabatic increase of the external voltage induces the following successive transition. In the low voltage, one has the region with a periodic oscillatory current of an asymmetric waveform, and then a possible region with a chaotic current oscillation follows. In these regions, non-ohmic branches are formed. In higher voltage, the region with a stable harmonic oscillatory current appears, having ohmic I-V branches. When there is a junction with a weaker j_c , the associated phase difference is easier to go into the rotating mode. Then the I-V characteristics have a quasi-periodic behavior in its non-ohmic region. The present analysis shows that voltage biased I-V characteristics reveals the importance of inter-layer coupling more strongly, and gives additional information to the current biased case.

Acknowledgements

This work was supported by the Special Research Grant in the Faculty of Engineering, Seikei University (H. M. and S. S.), and Grant-in-Aid for Scientific Research (C) from Japan Society for the Promotion of Science (T. K.).

References

- [1] R. Kleiner, F. Steimmeyer, G. Kunkel and P. Müller, Phys. Rev. Lett. 68, 2394 (1992).
- [2] R. Kleiner and P. Müller, Phys. Rev. B 49, 1327 (1994).
- [3] R. Kleiner, P. Müller, H. Kohlstedt, N. F. Pedersen, and S. Sakai, Phys. Rev. B 50, 3942 (1994).
- [4] S.Sakai, P. Bodin, and N. F. Pederson, J. Appl. Phys. 73, 24 (1993).
- [5] A. Yurgens, D. Winkler, N. V. Zavaritsky, and T. Claeson, Phys. Rev. B 53, R8887, (1996).
- [6] K. Tanabe, Y. Hidaka, S. Karimoto, and M. Suzuki, Phys. Rev. B 53, 9348 (1996).
- [7] M. Itoh, S. Karimoto, K. Namaekawa, and M. Suzuki, Phys. Rev. B 55, R12001, (1997).

- [8] C. Helm, Ch. Preis, F. Forsthofer, J. Keller, K. Schlenga, R. Kleiner, and P. Müller, Phys. Rev. Lett. 79, 737 (1997).
- [9] M. Sakai, A. Odagawa, H. Adachi, and K. Setsune, Physica C 299, 31 (1998).
- [10] K. Schlenga, R. Kleiner, G. Hechtfisher, M. Mößle, S. Schimit, P. Müller, Ch. Helm,, Ch. Preis, F. Forsthofer, J. Keller, H. L. Johnson, M. Veith, and E. Steinbeiß, Phys. Rev. B 57, 14518 (1998).
- [11] M. Tinkam, *Introduction to Superconductivity*, (McGraw-Hill, Inc. New York, 1996).
- [12] T. Koyama and M. Tachiki, Phys. Rev. B 54, 16183 (1996).
- [13] M. Machida, T. Koyama and M. Tachiki, Physica C 300, 55 (1998).
- [14] H. Matsumoto, S. Sakamoto, F. Wajima, T. Koyama and M. Machida, Phys. Rev. B 60 No.5 (to be published, 1999).
- [15] D. A. Ryndyk, Pis'ma Zh. Eksp. Teor. Fiz. 65, 755 (1997) [JETP Lett. 65, 791 (1997)].
- [16] D. A. Ryndyk, Phys. Rev. Letters 80, 3376 (1998).
- [17] P. Seidel, A. Pfuch, F. Schmidl, J. Scherbel and U. Hübner, Czech. J. Phys. 46, Suppl. S3, 1263 (1996).
- [18] Yu. I. Latyshev, S. -J. Kim and T. Yamashita, Pis'ma Zh. Eksp. Teor. Fiz. 69, 75 (1999) [JETP Letters B4, 84 (1999)].

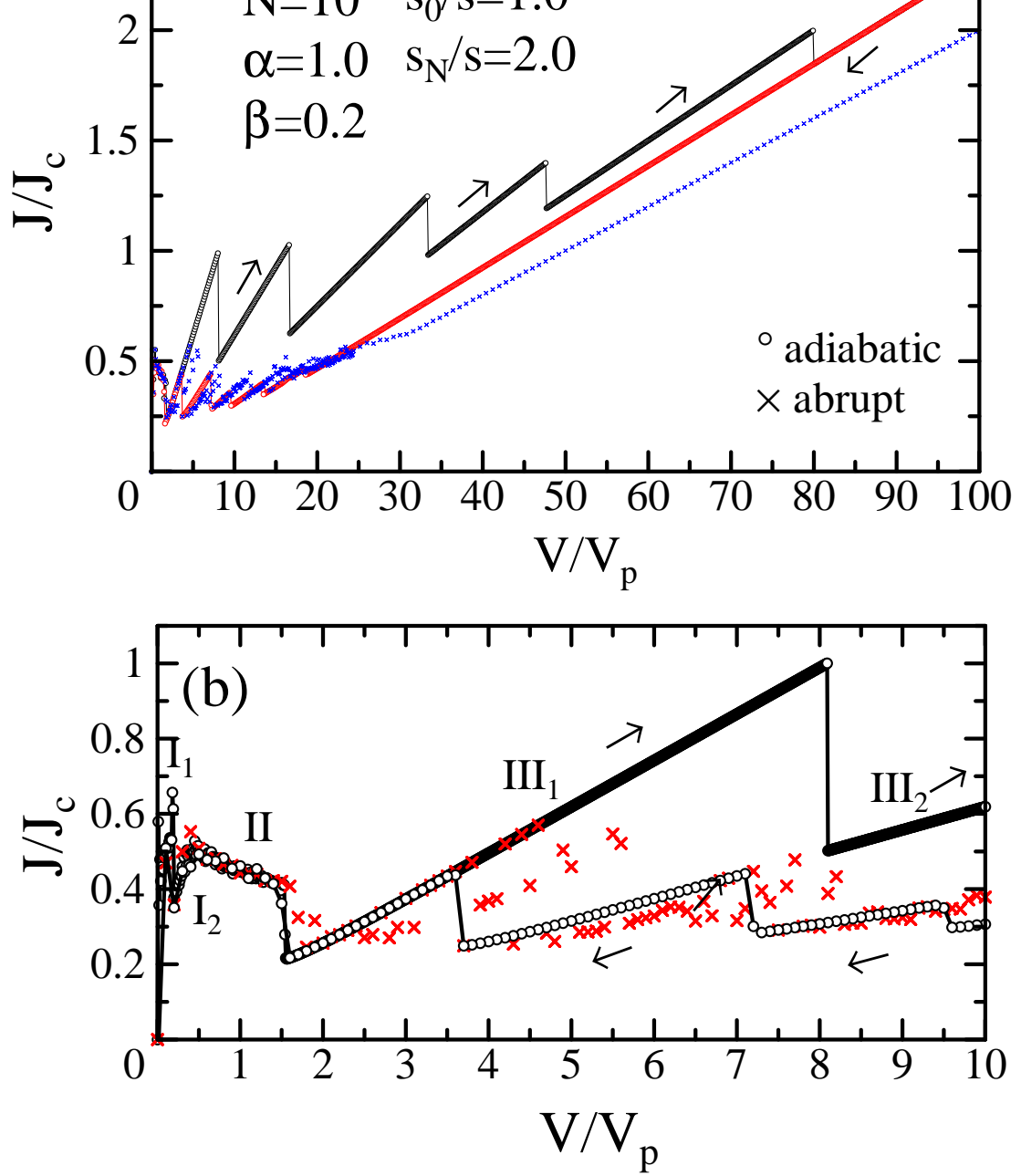


Fig. 1. I-V characteristics with an asymmetric boundary condition (a) for the wide range of V and (b) for the expanded low voltage region. The circles are for the adiabatic voltage change. The crosses are for the abrupt voltage application. Parameters are $\alpha = 1.0$, $\beta = 0.2$, $N = 10$, $\frac{s_0}{s} = 1.0$ and $\frac{s_N}{s} = 2.0$.

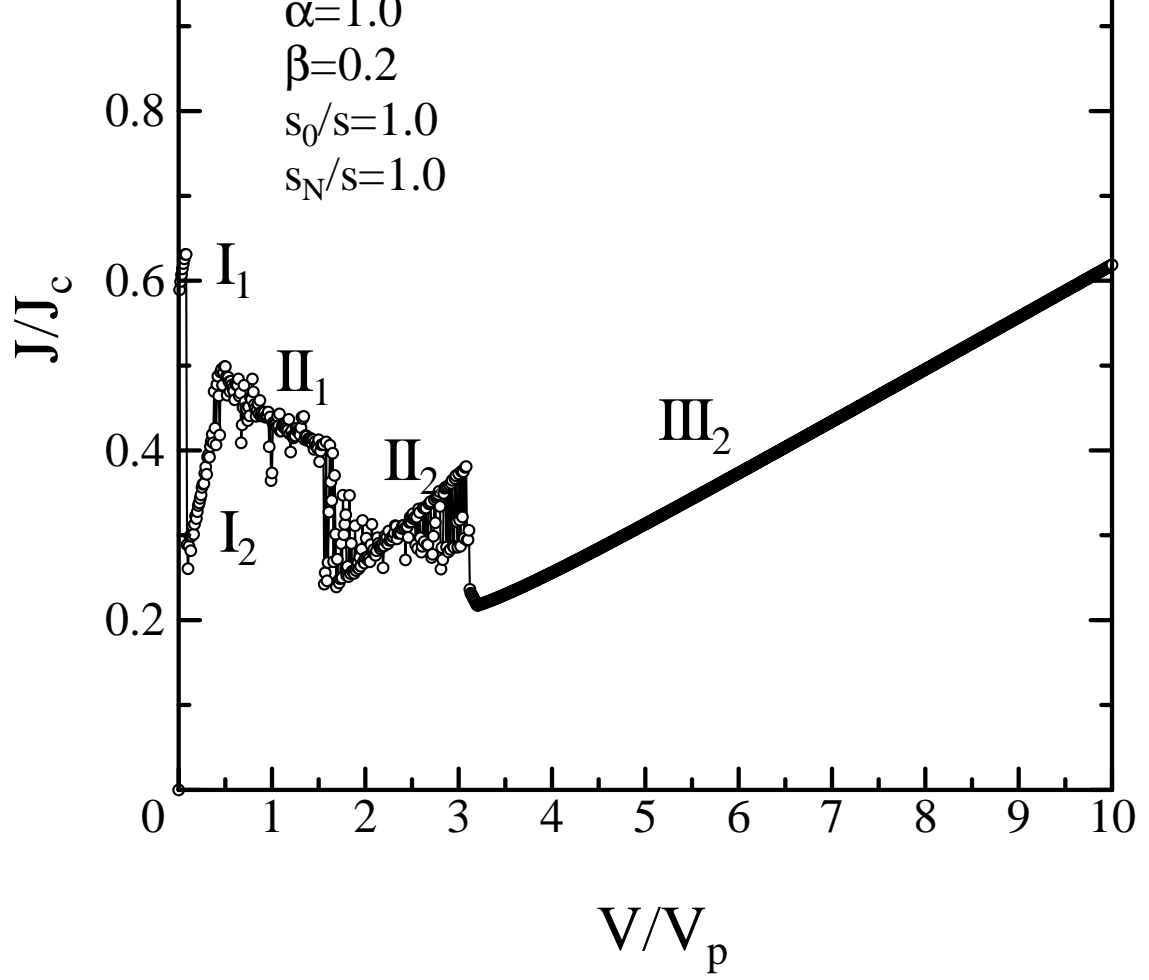


Fig. 2. I-V characteristics with a symmetric boundary condition. Parameters are $\alpha = 1.0$, $\beta = 0.2$, $N = 10$, $\frac{s_0}{s} = 1.0$ and $\frac{s_N}{s} = 1.0$.

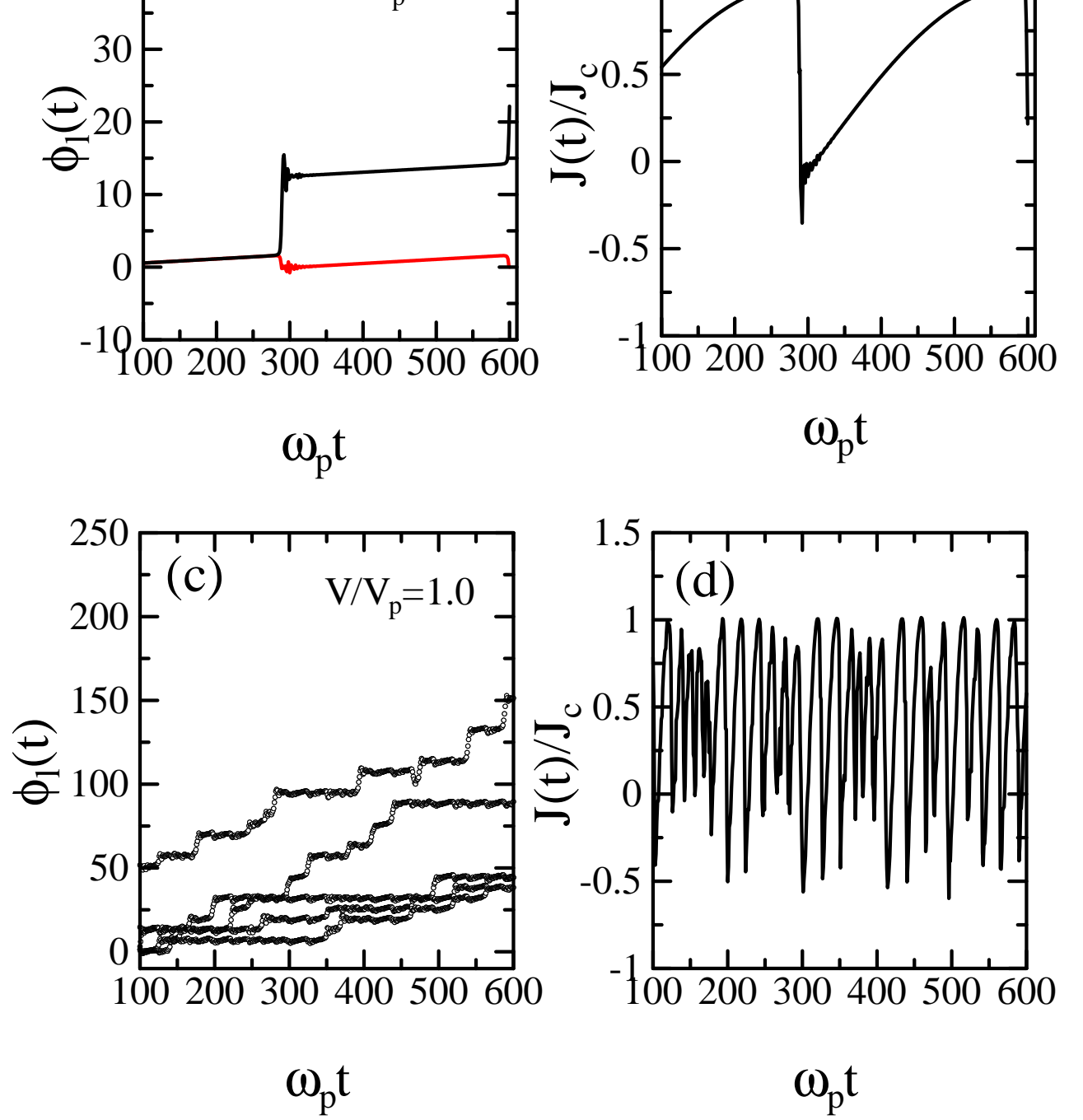


Fig. 3. Time dependence of $\varphi(l)$ and J/J_c for the branches I_1 ((a)-(b)) and Π_1 ((c)-(d))

Parameters are $\alpha = 1.0$, $\beta = 0.2$, $N = 10$, $\frac{s_0}{s} = 1.0$ and $\frac{s_N}{s} = 1.0$.

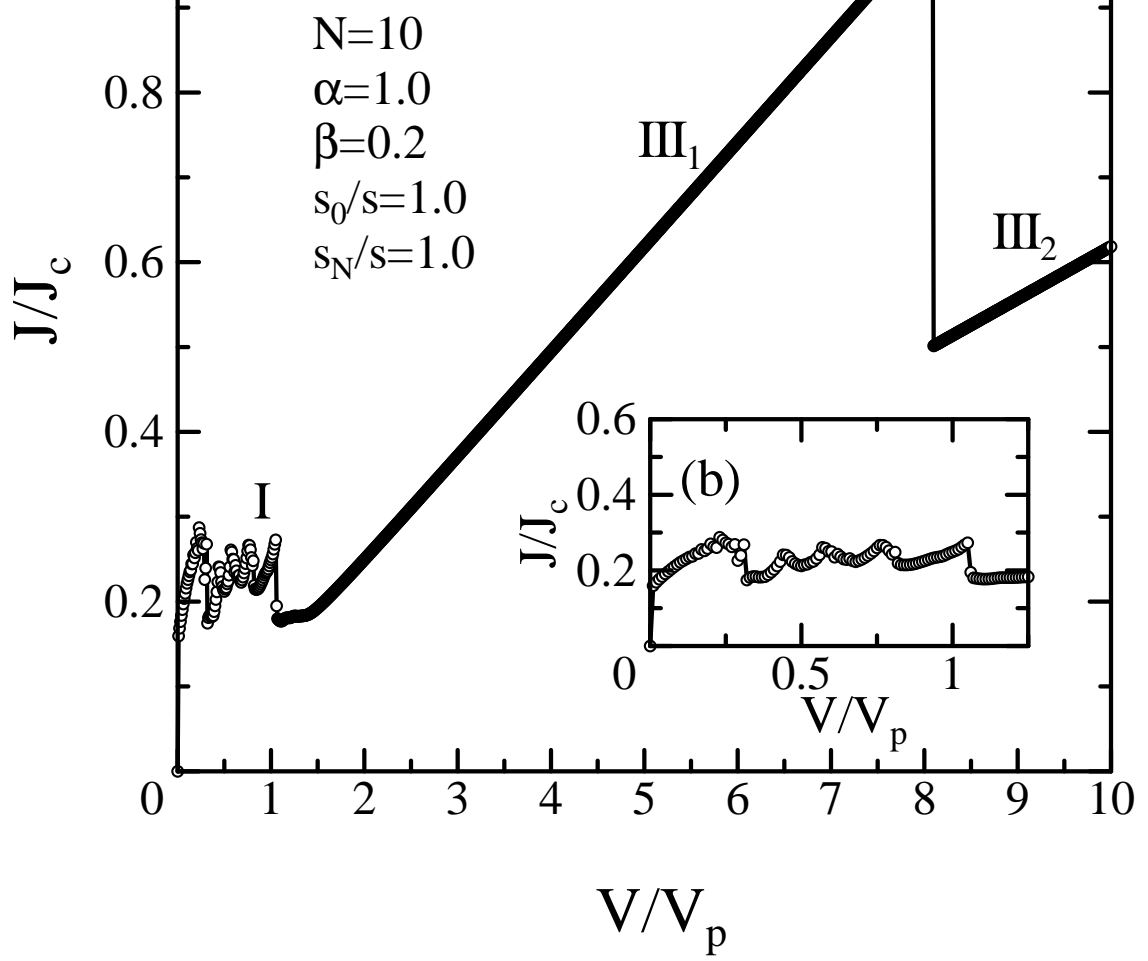


Fig. 4. I-V characteristics with a $j_c(l)$ -asymmetric boundary condition
Parameters are $\alpha = 1.0$, $\beta = 0.2$, $N = 10$, $\frac{s_0}{s} = 1.0$, $\frac{s_N}{s} = 1.0$, $j_c(0) = 0.5$ and $j_c(l) = 1.0$ ($l \neq 0$).